AUTOMATED CHANGE DETECTION IN LAND-COVER PATTERN USING REGION GROWING SEGMENTATION AND FUZZY VECTOR

Sang-Hoon Lee

Department of Industrial Engineering, Kyungwon University, Seongnam-si, Korea
shl@kyngwon.ac.kr

ISPRS WG IV/2 session

KEY WORDS: Remote Sensing, Change Detection, Segmentation, Fuzzy Membership

ABSTRACT:

This study has utilized a spatial region growing segmentation and a classification using fuzzy membership vectors to detect the changes in the images observed at different dates. Consider two co-registered images of the same scene, and one image is supposed to have the class map of the scene at the observation time. The method performs the unsupervised segmentation and the fuzzy classification for the other image, and then detects the changes in the scene by examining the changes in the fuzzy membership vectors of the segmented regions in the classification procedure. The algorithm has evaluated with simulated images and has then applied to a real scene of the Korean Peninsula using the KOMPSAT-1 EOC images. In the experiments, the proposed method has shown a great performance for detecting changes in land-cover.

1. INTRODUCTION

Change detection is the process of identifying differences in the state of an object or phenomenon by observing it at different times. Remote sensing data for change detection can be used based on the fact that changes must result in detectable changes in measurement or pattern. From the beginning of the remote sensing age, the ability to measure and analyze changes on the earth environment has been seen as one of the major advantages of remote sensing. For accurate change detection, many algorithms have been developed such as image differencing (Singh, 1989), principal component analysis (Buruzzone and Prieto, 2000), change vector analysis (Buruzzone and Prieto, 2002), Markov random fields (Gong, 1993), neural network (Dai and Khorram, 1998), feature extraction (Zeng *et al*., 2002). This study proposes an effective method for detecting land-cover changes in remote sensing using a regional growing segmentation and fuzzy classification.

The spatial region growing algorithm was suggested for image segmentation in Lee and Crawford (2005). The region-growing algorithm uses the hierarchical clustering procedure, which operates the step-by-step merging of small clusters into larger ones based on similarity measures between all pairs of candidates being considered for merging. The algorithm is designed to do merging within spatial adjacency under the hierarchical constraint and finally partition the image as any number of regions which are sets of spatially contiguous pixels so that no union of adjacent regions is statistically uniform. The fuzzy classification is an EM (expected maximization) iterative approach based on mixture probability distribution (Liang *et al.*, 1992). Under the assumption of a double compound stochastic image process, given an initial class map, this approach iteratively computes the fuzzy membership vectors in the E-step and the maximum likelihood estimates of class-related parameters in the M-step, and when satisfying a convergence condition, generates the optimal class map according to the fuzzy membership vectors. In the double compound image model, an MRF (Kindermann and Snell, 1982) is used to quantify the spatial continuity or smoothness probabilistically, that is, to provide a type of prior information on the region-class process for image classification.

Consider two co-registered images of the same scene observed at different times. One image is supposed to have the class map of the scene at the observation time. The method performs the unsupervised segmentation and the fuzzy classification for the other image, and then detects the changes in the scene using the results of fuzzy classification. The most important advantage of the proposed detection technique is that it can apply to the comparison between the images acquired from sensors of different spectral ranges and/or with different number, position, and width of spectral bands. The algorithm has evaluated with simulated images.

2. SPATIAL REGION GROWING SEGMENTATION

One essential structural characteristic involves hierarchy of scene information. Under the constraint of the hierarchical structure, it is then possible to determine natural image segments by combining hierarchical clustering with spatial region growing. Hierarchical clustering (Anderberg, 1973) is an approach for step-by-step merging of small clusters into larger ones. Clustering algorithm utilize a similarity/dissimilarity measure that is computed between all pairs of candidates being considered for merging, a rule for selecting the pairs to be merged, and a rule for "cutting" the

hierarchical tree. The computational efficiency of hierarchical clustering segmentation is mainly dependent on how to find the best pair to be merged. The closest neighbor of region j is defined as

$$\mathrm{CN}(j) = \arg\min_{k \in \mathbf{R}_j} d(j,k)$$

where $d(j,k)$ is the dissimilarity measure between regions j and k, and $\mathbf{R}_j$ is the index set of regions considered to be merged with region j. The pair of regions is then defined as MCN iff $k = \mathrm{CN}(j)$ and $j = \mathrm{CN}(k)$. It is easily shown that the best pair is one of the MCNs. In Lee and Crawford (2005), the search for the best pair is limited in the set of MCNs the segmentation performs to be merged among all the MCN pairs. But, this approach updates the set of MCN pairs at every iteration, and may then result in computational inefficiency for the segmentation. This method links two adjacent regions that are a MCN pair, using "closest neighbor chain (CN-chain)." It does not require the search of the best pair and the update of the set of MCN pairs. Both the techniques use a multi-window strategy of boundary blocking operation (Lee, 1990) to alleviate the memory problem and improve the computational performance of the algorithm.

3. FUZZY CLASSIFICATION USING MRF

It is natural that neighboring pixels with closer intensity levels have a higher probability of being the same class. Based on this idea, spatial continuity can be quantified for image processes with the pair-potentials that are functions of a distance between the neighboring pixels in the mean intensity $\mu(\omega)$, which is a mapping function of ω into real intensity values. The energy function of the MRF is specified in terms of a quadratic function of $\mu(\omega)$ to define the probability structure of the region-class process for the segmentation: if $[\mathbf{v}]^2$ denotes the vector whose elements are squared values of each element of vector $\mathbf{v}$,

$$E_p(\omega) = \sum_{(i,j) \in C_p} \alpha'_{ij} [\mu(\omega_i) - \mu(\omega_j)]^2$$

where ω_i is the class of the ith pixel, $\mu(\omega_i)$ is the mean intensity vector of class ω_i, and α_{ij} is a non-negative coefficient vector, which represents the "bonding strength" of the ith and the jth pixels.

Without generalization, the observed intensity processes are usually assumed to be Gaussian, and using the MRF associated with the energy function for region-class processes, the posterior joint distribution of the class vector ω and the observed intensity process $\mathbf{X}$ is then

$$f(\mathbf{X},\omega) = f(\mathbf{X} \mid \omega) f(\omega) \propto \exp\left\{-[\mathbf{X} - \mu(\omega)]' \boldsymbol{\Sigma}^{-1}(\omega)[\mathbf{X} - \mu(\omega)] - E_p(\omega)\right\}$$

where $\boldsymbol{\Sigma}(\omega)$ is the covariance matrix of the observed intensity process. If $\boldsymbol{\Omega}$ is the set of all possible class configurations,

$$\int_{\Omega} f(\omega) d\omega = 1$$

and the conditional probability is then

$$f(\mathbf{X} \mid \omega) = \sqrt{2\pi |\boldsymbol{\Sigma}|}^{-1} \exp\left\{-[\mathbf{X} - \mu(\omega)]' \boldsymbol{\Sigma}^{-1}(\omega)[\mathbf{X} - \mu(\omega)] - E_p(\omega)\right\}$$

Consider a problem classifying M regions in K classes. The data set of region m, $\mathbf{X}_m = \{\mathbf{x}_j, j \in J_m\}$, where J_m is the index set of pixels in region m and $\mathbf{x}_j$ is the data vector of pixel j, is associated with an unobserved image class k, which is to be estimated. This association between $\mathbf{X}_m$ and class k can be specified completely with an unobserved indicator vectors, $\mathbf{s}_m = \{s_{km}, k = 1, \cdots, K\}$. In ideal situation, the kth element of $\mathbf{s}_m$ has unit value and all the other elements are zero if region m belongs to class k. The mixture probability distribution of the complete data set $\mathbf{Z} = \{\mathbf{X}_m, \mathbf{s}_m\}$ is then expressed as

$$F(\mathbf{Z} \mid \mathbf{W}, \Theta) = \prod_m \prod_k w_k^{s_{km}} f_k^{s_{km}}(\mathbf{X}_m \mid \boldsymbol{\theta}_k)$$

where $\mathbf{W} = \{w_k\}$ represents the weights of the components $\{f_k\}$ in the mixture distribution, $\sum_k w_k = 1$, and $\boldsymbol{\Theta} = \{\boldsymbol{\theta}_k\}$ is the set of parameters that define the classes. The fuzzy classification procedure calculates the indicator variables $\{s_{km}\}$ in the E-step, and the likelihood of $\mathbf{W}$ and $\boldsymbol{\Theta}$ is maximized in the M-step using $\{s_{km}\}$ estimated in the E-step. In this study, under the assumption of additive Gaussian image model, EM iterative approach computes the fuzzy vector. Figure 1 shows the EM iterative approach to compute the fuzzy vectors.

(E-step)

$$s_{kj}^{(h)} = \frac{w_k^{(h)} f_k(\mathbf{x}_j \mid \Theta^{(h)})}{\sum_i w_i^{(h)} f_i(\mathbf{x}_j \mid \Theta^{(h)})} \quad \text{and} \quad \sum_k s_{kj}^{(h)} = 1$$

$$f_k(\mathbf{x}_j \mid \Theta^{(h)}) = \left(\sqrt{2\pi |\Sigma_k^{(h)}|}\right)^{-1} \exp^{-1}\left(\Delta_q + \Delta_p\right)$$

$$\Delta_q = \frac{1}{2}\left(\mathbf{x}_j - \mu_k^{(h)}\right)' \Sigma_k^{(h)^{-1}} \left(\mathbf{x}_j - \mu_k^{(h)}\right)$$

$$\Delta_p = \sum_{(i,j) \in C_p} \alpha'_{ij} \sum_{m=1}^{K} s_{mj}^{(h)} \left[\mu_k^{(h)} - \mu_m^{(h)}\right]^2$$

(M-step)

$$w_k^{(h+1)} = \frac{1}{N} \sum_j s_{kj}^{(h)}$$

$$\mu_k^{(h+1)} = \frac{1}{N w_k^{(h+1)}} \sum_j s_{kj}^{(h)} \mathbf{x}_j$$

$$\Sigma_k^{(h+1)} = \frac{1}{N w_k^{(h+1)}} \sum_j s_{kj}^{(h)} \left(\mathbf{x}_j - \mu_k^{(h+1)}\right)' \left(\mathbf{x}_j - \mu_k^{(h+1)}\right)$$

Figure 1. EM iteration.

4. DETECTION ALGORITHM

Consider two co-registered images of the same scene observed at different times. One image is supposed to have the class map

of the scene at the observation time. The proposed detection scheme is to find the changes in the other image based on the class map. The other image will be referred to as the observed image, and the given class map as the reference class configuration. The changes in the observed image are detected by the following procedure:

1) Segment the observed image using the spatial region growing algorithm.
2) Partition the segmented regions that consist of two or more classes such that all the resultant regions have a uniform class. For example in Figure 2, the class map has two classes and the observed image has been partitioned with 9 segments, resulting in 17 segments (9 segments of class 1 and 8 segments of class 2).
3) Initialize the indicator vectors for the fuzzy classification such that the element associated with the region class of the reference configuration has unit value and all the others are zero.
4) Perform the classification and generate the final indicator vectors for the regions.
5) Detect the changes in the class configuration of the regions by comparing the initial class configuration and the resultant indicator vectors.

Figure 3 outlines the proposed detection algorithm.

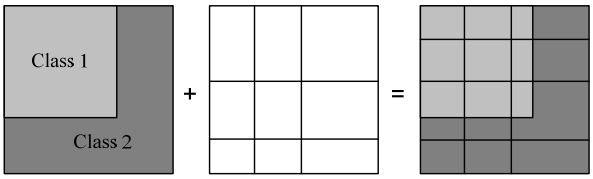

Figure 2. Example of combining class map and region segmentation.

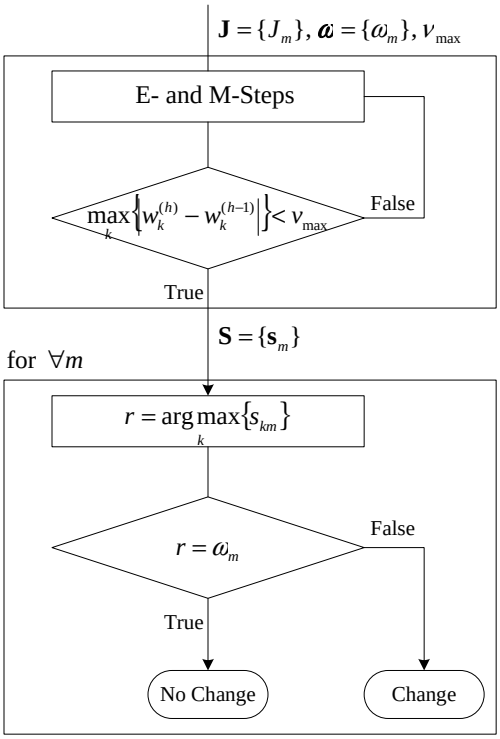

Figure 3. Detection algorithm.

5. EXPERIMENT

Single- and 3-band 8-bit simulation images have been generated using a simple pattern, which may represent a remotely-sensed environmental scene, by adding white Gaussian noise, whose variance is pixel-independent and region-dependent. Thus, the region-class process is characterized by the mean and variance of intensity values. In order to represent varying noise levels in the simulation images, the signal-to-noise ratio (SNR) is defined as the ratio of the smallest intensity-level difference to the average noise standard deviation. For computational convenience, the SNR values are the same for all bands, the variances of all region-classes are identical, and the differences between contiguous levels in order of mean intensity are constant. The proposed algorithm has first been evaluated with the simulation data. This study generated simulated observation images with two levels of SNR (1.0 and 2.0 for single band and 0.5 and 1.0 for three bands) using the additive Gaussian image model. Figures 4-a and -b are the maps of the reference class configuration and change-areas for the experiments respectively. The pattern used to simulate the observed images and an example of simulated single-band observation with SNR = 1.0 are shown in Figures 4-c and –d respectively. Figure 4-e is the map of detected change-areas which results from applying the proposed detection scheme to the simulation data of Figure 4-d. Tables 1 and 2 contain the results of the experiments for the 4 sets of simulation data. As shown in the tables, the error rates are less than 1% in almost all changes for the single-band data of SNR = 1.0 and both the 3-band data.

6. CONCLUSION

The most intuitive technique to detect change is simple differencing followed by threshold. Change at a pixel is detected if the difference in measurement levels of the corresponding pixels in consecutive frames exceeds a preset threshold. This technique is computationally efficient, but the result is very susceptible to noise and it is not suitable for applications of time varying imagery. The experimental results show that the proposed method is quite effective for the change detection using the images observed at different dates. For the comparison between the images acquired from sensors of different spectral ranges and/or with different number, position, and width of spectral bands, the approach, which is based on classification, is more appropriate than the conventional techniques based on the intensity values.

ACKKNOWLEDGEMENTS

This research was supported by partially a grant(07KLSGC03) from Cutting-edge Urban Development – Korean Land Spatialization Research project funded by Ministry of Land, Transport and Maritime Affairs of Korean government and partially Kyungwon University.

REFERENCES

Anderberg, M.R, 1973. *Cluster Analysis for Application*, Academic Press, NY.

Bruzzone, L. and D. F. Prieto, 2000. Automatic analysis of the difference image for unsupervised change detection, *IEEE Trans. Geosci. Remote Sensing*, 38, pp. 1171-1182

Bruzzone, L. and D. F. Prieto, 2002. An adaptive semi-parametric and context-based approach to unsupervised change detection in multitemporal remote sensing images *IEEE Trans. Image Processing*, 11, pp. 452-466

Dai, X. and S. Khorram, 1998. The effects of image misregistration on the accuracy of remotely sensed change detection, *IEEE Trans. Geosci. Remote Sensing*, 61, pp. 313-320.

Gong, P., E. F. LeDrew, and J. R. Miller, 1992. Registration-noise reduction in difference images for change detection, *Int. J. Remote Sens.*, 13, pp. 773-779

Kindermann, R. and J.L. Snell, 1982. *Markov Random Fields and Their Application*, Amer. Math. Soc., Providence, R. I..

Lee, S-H, 1990, An Unsupervised Hierarchical Clustering Image Segmentation and an Adaptive Image Reconstruction System for Remote Sensing, Ph. D. Dissertation, University of Texas at Austin.

Lee, S-H. and M. Crawford, 2005. Unsupervised multistage image classification using hierarchical clustering with a bayesian similarity measure, *IEEE Trans. Image proc.*, 14, pp. 312-320.

Liang, Z, R.J. Jaszczak and R.E. Coleman, 1992. Parameter Estimation of Finite Mixture Using the EM Algorithm and Information Criteria with Application to Medical Image Processing, *IEEE Trans. Nucl. Sci.*, 39, pp. 1126-1133.

Singh, A., 1989. Digital change detection techniques using remotely-sensed data, *Int J. Remote Sens.*, 10, pp. 989-1003

Zeng, Y., J. Zhang, and G. Wang, 2002. Change detection of guildings using high resolution remotely sensed data, *Proc. Int. Sym. Remote Sensing*, pp.530-535.

Table 1. Error Rates of Change Detection for Single-Band.

	SNR = 1.0				SNR = 2.0			
	1	2	3	Error Rate	1	2	3	Error Rate
1	306725*	1828	320	0.007	307965*	879	29	0.003
1	1037	10788	109	0.096	29	11905	0	0.002
1	35	19	14047	0.004	1	0	14100	0.000
2	18548	715	0	0.037	19103	160	0	0.008
2	6090	396390*	1844	0.020	969	402533*	822	0.004
2	4	1813	16936	0.097	0	257	18496	0.014
3	12254	199	58	0.021	12437	66	8	0.006
3	10	10389	2528	0.161	0	12807	110	0.009
3	107	1396	244397*	0.006	32	624	245244*	0.003

Table 2. Error Rates of Change Detection for 3 Bands

	SNR = 1.0				SNR = 2.0			
	1	2	3	Error Rate	1	2	3	Error Rate
1	308729*	81	63	0.000	308700*	159	14	0.001
1	17	<u>11863</u>	54	0.006	24	<u>11910</u>	0	0.002
1	9	1	<u>14091</u>	0.001	3	0	<u>14098</u>	0.000
2	<u>19094</u>	169	0	0.009	<u>19148</u>	115	0	0.006
2	1920	400443*	1961	0.010	1317	402068*	939	0.006
2	0	239	<u>18514</u>	0.013	0	110	<u>18643</u>	0.006
3	<u>12453</u>	44	14	0.005	<u>12502</u>	3	6	0.001
3	7	<u>12441</u>	469	0.037	0	<u>12718</u>	199	0.015
3	67	150	245683*	0.001	7	197	245696*	0.001

*: Number of pixels of the areas that were actually not changed in the original pattern and were not detected as a change area.

Underline: Number of pixels of the areas that were actually changed in the original pattern and were correctly detected as a change area

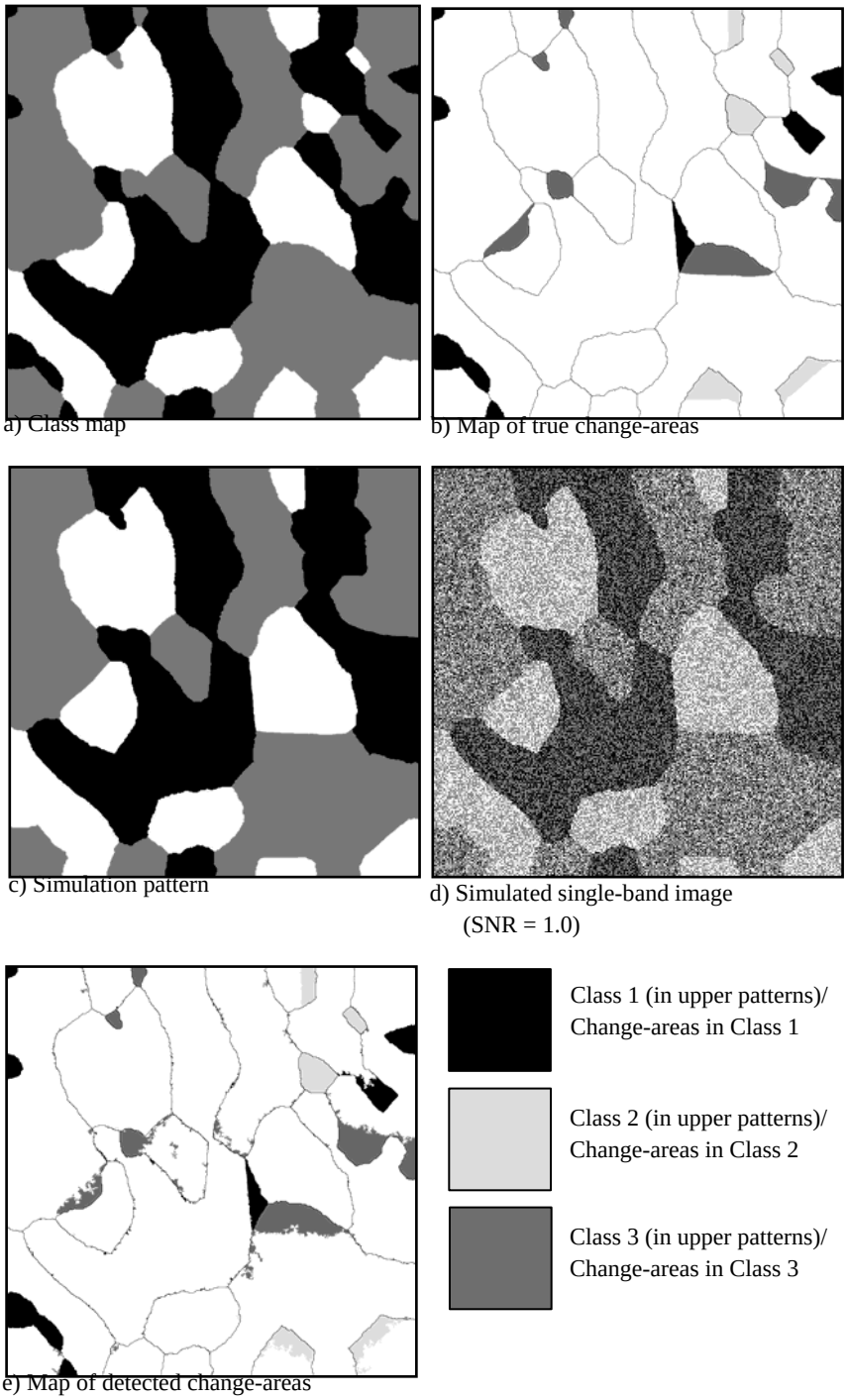

Figure 4. Experimental data and results.